Electrospinning of Poly(L-lactide) Nanofibers Encapsulated with Water-Soluble Fullerenes for Bioimaging Application

Wanyun Liu,[§,†] Junchao Wei,[§,†] Yiwang Chen,*[,†] Ping Huo,[†] and Yen Wei[‡]

[†]Department of Chemistry/Institute of Polymers, Nanchang University, 999 Xuefu Avenue, Nanchang 330031, China
[‡]Department of Chemistry, Tsinghua University, Beijing 100084, China

Ⓢ *Supporting Information*

ABSTRACT: Photoluminescent fullerene nanoparticles/nanofibers have potential applications in bioimaging. A novel fluorescent nanofibrous material, consisting of fullerene nanoparticles and poly(L-lactide) (PLLA), was fabricated via a simple electrospinning method, and the composite nanofibers were characterized by various techniques such as scanning electron microscopy (SEM), laser scanning confocal microscopy (LSCM), and transmission electron microscopy (TEM). The nanofibers were uniform, and their surfaces were reasonably smooth, with the average diameters of fibers ranging from 300 to 600 nm. The fullerene nanoparticles were encapsulated within the composite nanofibers, forming a core–shell structure. The nanofiber scaffolds showed excellent hydrophilic surface due to the addition of water-soluble fullerene nanoparticles. The composite nanofibers used as substrates for bioimaging *in vitro* were evaluated with human liver carcinoma HepG2 cells, the fullerene nanoparticles signal almost displayed in every cell, implying the potential of fluorescent fullerene nanoparticles/PLLA nanofibers to be used as scaffolds for bioimaging application.

KEYWORDS: fullerene, nanoparticles, electrospinning, nanofiber, tissue engineering, bioimaging
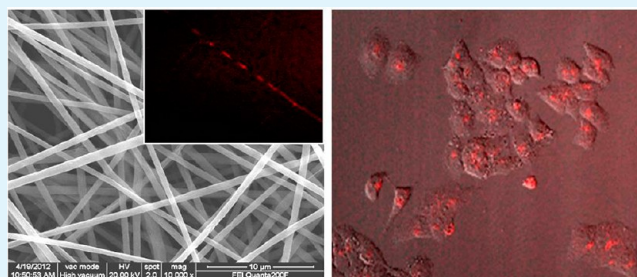
INTRODUCTION

Fluorescent nanoparticles have recently gained widespread interest due to their size or surface dependent photoluminescence, subsequent functionality, and biocompatibility. The fluorescent nanoparticles have been used for various biomedical applications such as diagnostics and therapeutics due to their unique capabilities and their low side effects.[1−5] Conventional fluorescent nanoparticles, including semiconductor quantum dots and dye-doped fluorescent nanoparticles, are widely used as fluorophores for biological imaging and clinical assay applications. However, they are facing some major limitations such as toxic effects of semiconducting quantum dots, low absorption coefficients, weak signal, and poor photobleaching resistance of organic dyes.[6−8] Recently, much effort has been concentrated on the design and development of novel water-soluble fullerenes, making them available and favorable for bioimaging studies such as cellular uptake, biodistribution, and organ/target specific binding tests. Fullerene fluorescent nanoparticles have offered a high potential for bioimaging application due to their unique properties such as nonblinking fluorescence emission, excellent water solubility, high cell permeability, and good biocompatibility.[9−11]

Nanofibers exhibit a range of unique features and properties, such as the simplicity of fabrication method, the diversity of materials suitable for processing into fibers, high surface area, and a complex porous structure, and they also have molecular-level alignment.[12−16] In recent years, researchers have used electrospinning technique to fabricate ultrafine fibers with diameters in nanometer range for wound dressing, biosensor, tissue engineering scaffolds, and drug delivery applications.[17−21] Implanting biodegradable polymer electrospun nanofibers in the tumor bed has promising prospects used in postoperative local chemotherapy. The advantages of this method are not only achievement of a high local drug concentration by using a small amount of drug but also minimization of severe side effects.[22,23] Especially, if implanting the nanofibers encapsulated with fluorescent nanoparticles in the tumor bed for bioimaging, then we can observe the tumor cell morphology and changes at anytime. Nanofiber scaffolds is a potential tissue engineering tool as it can be fabricated and shaped to fill anatomical defects. However, to the best of our knowledge, there were few reports on electrospinning of nanofibers encapsulated with fluorescent nanoparticles for bioimaging application.[24]

PLLA is biodegradable aliphatic polyester used in a variety of biomedical applications. It has a number of important characteristics such as biocompatibility and biodegradability, tunable degradation rate, and high solubility in organic solvents, and thus it exhibits good potential in formulating drug delivery systems. In addition, PLLA has attractive mechanical properties and excellent shaping and molding properties and can be fabricated into porous nanofibers and many other types of structures. The diverse architectures can be designed to provide
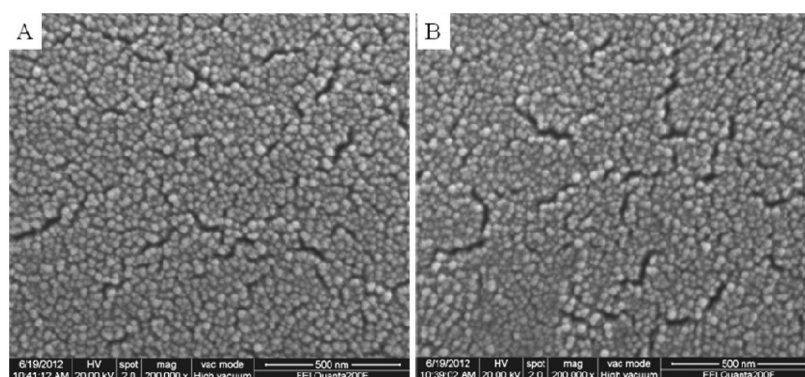
Figure 1. SEM images of fullerene nanoparticles: (A) C_{60}-TEGs and (B) C_{70}-TEGs.

growth factors, drugs, therapeutics, and genes to stimulate tissue regeneration. Therefore, nanoscale fibers of PLLA have attracted the interest of numerous researchers.[25−27]

In this study, PLLA nanofibers encapsulated with water-soluble fullerene nanoparticles were prepared via blend electrospinning method. The electrospun nanofibers used as substrates for bioimaging were evaluated with human liver carcinoma HepG2 cells *in vitro*, and the fullerene nanoparticles released from the fibers could penetrate into the cells, displaying fluorescence images almost in every cell. This work was expected to exploit a novel fluorescent composite nanofiber material and accelerate their use in bioimaging application.

■ MATERIALS AND METHODS

Materials. C_{60} fullerene and C_{70} fullerene were purchased from Aldrich. Tetraethylene glycol (TEG), lithium hydroxide, and MTT (3-(4,5-dimethylthiazolyl-2)-2,5-diphenyl tetrazolium bromide) were purchased from Aladdin reagent and were used without further purification. Poly(L-lactide) (PLLA) (molecular weight 100K) was purchased from Shandong Jianbao Biomaterials Ltd. (Jinan, China). Human liver carcinoma HepG2 cell was purchased from Shanghai cell center (Chinese Academy of Sciences). Other reagents were commercially available and used as received.

Preparation of Water-Soluble Fullerene Nanoparticles. Water-soluble fullerene nanoparticles C_{60}-TEGs and C_{70}-TEGs were prepared according to the literature.[9] Briefly, C_{60} fullerene or C_{70} fullerene solution (10 mL toluene) at a concentration of 1 mg/mL was added to 10 mL of tetraethylene glycol (TEG). Lithium hydroxide (40 mg) was then added to the mixture of fullerene and TEG, and the solution turned from pink to dark brown within 10 min. After having been stirred for 20 h, the resulting fullerene nanoparticles were precipitated by adding excess ethyl acetate (EA). The precipitates were collected by centrifugation and redispersed in ethanol. The product was washed by repeating the dispersion-precipitation process several times and then lyophilized to obtain water-soluble fullerene nanoparticles powders.

Preparation of PLLA Nanofibers Encapsulated with Water-Soluble Fullerene Nanoparticles. PLLA was dissolved in the blend solvents of chloroform and DMF (volume ratio is 3:1) by using a bath sonicator (KQ-100, China) to prepare 10 wt.% solution, respectively. 5-20 wt.% of water-soluble fullerene nanoparticles with respect to the used polymer were added into the polymer solution by continuous stirring. The mixture solution was then immediately electrospun. The nanofibers were collected on a target drum, which was placed at a distance of 11−13 cm from the syringe tip (inner diameter 22 μm). A voltage of 23−26 KV was applied to the syringe tip by a high voltage power supply, and the flow rate of the solution was 15 μL/min. All electrospinning experiments were carried out at about 25 °C in air. The nanofibers were dried in vacuum for 72 h at 37 °C to remove the residual solvent. The blank fiber without nanoparticles was fabricated by the same method.

Characterization of the Fullerene Nanoparticles and Electrospun Composite Nanofibers. The photoluminescence (PL) spectra of fullerene nanoparticles and electrospun PLLA nanofibers loaded with fullerene nanoparticles were determined by a fluorescence spectrophotometer (Hitachi F-7000). For fluorescence emission spectra, the excitation wavelength was 350 nm, and the excitation bandwidth was 5.0 nm. The spectra were recorded from 450 to 700 nm with a scanning rate 1200 nm/min. A scanning electron microscope (SEM, FEI Quanta 200SEM) was used to observe the surface morphologies and diameters of fullerene nanoparticles and electrospun PLLA nanofibers loaded with fullerene nanoparticles at an accelerating voltage of 20 kV. Each sample was sputter-coated with aurum for analysis. The diameter of the fullerene nanoparticles and fibers were measured from the SEM micrographs. Laser scanning confocal microscopy (LSCM: ZEISS LSM 710, Germany) was used to evaluate the distribution of fullerene nanoparticles in the electrospun nanofibers. Interface nanostructure of composite fibers was analyzed using transmission electron microscopy (TEM) (JEOL-2100F) at 150 kV. Samples for TEM were prepared by directly depositing electrospun nanofibers onto carbon-coated copper grids.

Water contact angles of nanofiber mats were measured using a contact angle instrument (JC2000A). During the measurements, the samples of nanofiber mats cut into square pieces with the size of 1 cm^2 were placed on a testing plate. Subsequently, distilled water (0.03 mL) was carefully dropped onto the prepared mats, and the static images were taken at various time periods (1 s and 30 s). Five measurements at different surface locations were carefully conducted for each sample, and the reported data were the mean value.

Mechanical properties of different nanofiber mats were determined using a SANS WDW universal test system with electronic data evaluation on specimens of 40 × 10 mm with a thickness in the range of 65 to 75 μm. At least five samples were tested for each type of electrospun nanofiber mats, and average values were reported.

***In Vitro* Biological Imaging and Cell Viability Assay.** The potential use of the PLLA electrospun nanofibers loaded with water-soluble fullerene nanoparticles as substrates for bioimaging application was evaluated with human liver carcinoma HepG2 cells *in vitro*. HepG-2 cells were cultured in Dulbecco's Modified Eagle's Medium (DMEM) supplemented with 10% FBS and 1% penicillin/streptomycin at 37 °C in a humidified incubator with 5% CO_2, and the culture medium was replaced once every 2 days. After reaching 80% confluence, the cells were detached by 0.25% Trypsin-EDTA, and viable cells were counted by hemocytometer.

For bioimaging, the HepG-2 cells (5×10^3 cells/well) were seeded onto pieces of nanofiber mats (1 cm × 1 cm) sterilized by UV radiation for 3 h in 6-well plates. Then, HepG-2 cells were cultured in DMEM supplemented with 10% FBS, 1% penicillin/streptomycin at 37 °C, 5% CO_2, and a humidity atmosphere. After cultured for 1, 2, and 3 days, the fluorescence images of the cells were obtained using a laser scanning confocal microscopy (LSCM: ZEISS LSM 710, Germany).

The cell viabilities of fullerene nanoparticles (C_{60}-TEGs, C_{70}-TEGs) and PLLA electrospun fibers encapsulated with fullerene nanoparticles

against HepG-2 cells were assessed using MTT (3-(4,5- dimethylth-iazol-2-yl)-2,5-diphenyltetrazolium bromide). HepG-2 cells (8×10^3) were plated in 24-well plates and incubated with 1.0 mg/mL fullerene nanoparticles; 1.0 mg composite nanofibers contained various concentrations of fullerene nanoparticles and blank fiber using test cells as control groups, respectively. After 48 h, the cells were treated with MTT according to the manufacturer's protocol. The absorbance values were recorded at approximately 595 nm. The signals were averaged from three values obtained from different wells.

■ RESULTS AND DISCUSSION

Characterization of the Fullerene Nanoparticles. The SEM micrographs of C_{60}-TEGs and C_{70}-TEGs were shown in Figure 1. The images revealed that the nanoparticles showed uniformly spherical shape. The average size of fullerene nanoparticles C_{70}-TEGs was determined to be about 16.5 nm, which was larger than that of C_{60}-TEGs (about 15.0 nm).

To investigate the photophysical properties of fullerene nanoparticles C_{60}-TEGs and C_{70}-TEGs, the photoluminescence (PL) spectra of C_{60}-TEGs and C_{70}-TEGs dissolved in water were shown in Figure 2. The emission spectra of the C_{60}-TEGs
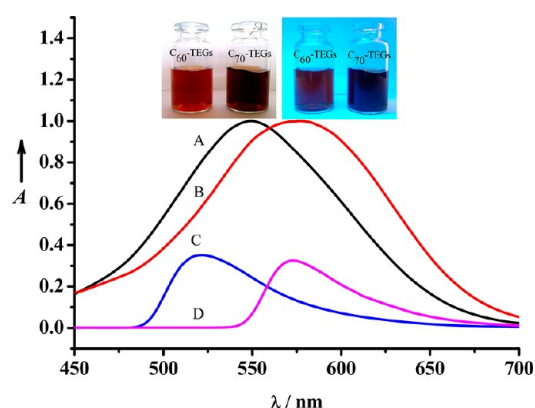

Figure 2. Photoluminescence spectra of fullerene nanoparticles and PLLA nanofibers encapsulated with fullerene nanoparticles: (A) C_{60}-TEGs, (B) C_{70}-TEGs, (C) PLLA nanofibers encapsulated with 10 wt. % C_{60}-TEGs, and (D) PLLA nanofibers encapsulated with 10 wt.% C_{70}-TEGs. Insert image: photographs of fullerene nanoparticles solutions (1 mg/mL) under white light (left) and under a UV lamp (365 nm) (right).

and C_{70}-TEGs exhibited maximum emission wavelength at 550 nm and 575 nm (under 350 nm excitation). Compared with C_{60}-TEGs, the color of C_{70}-TEGs solution was darker, the maximum emission wavelength was longer, and the photoluminescence intensity was stronger.

From these results, it could be concluded that water-soluble fullerene nanoparticles C_{60}-TEGs and C_{70}-TEGs were prepared successfully, and the luminescence properties of fullerene

nanoparticles were useful in potential for bioimaging applications.[9]

Characterization of the Electrospun Composite Nanofibers. The photoluminescence spectra of the PLLA nanofibers encapsulated with fullerene nanoparticles was shown in Figure 2. The observed typical PL emission of fullerene nanoparticles could confirm that the fullerene nanoparticles were encapsulated by the electrospun composite nanofibers. Compared to the fluorescence efficiency of fullerene nanoparticls in solution state, the fluorescence efficiency in the nanofibers was lower and maximum emission wavelength blue-shifting, implying the fullerene nanoparticles were well incorporated and uniformly dispersed into the PLLA nanofibers.

The SEM micrographs of the nanofibers were shown in Figure 3 and Figure S1 (in the Supporting Information, blank PLLA nanofiber and PLLA nanofiber encapsulated with 10 wt. % of C_{70}-TEGs). The electrospun nanofibers represented an identical morphology of PLLA fibers to those containing fullerene nanoparticles. The nanofibers were uniform, and their surfaces were reasonably smooth, with the average diameters of fibers ranging from 300 to 600 nm. The average diameters of the fibers contained 0 wt.%, 5 wt.%, 10 wt.%, and 20 wt.% C_{60}-TEGs and were about 300, 330, 480, and 570 nm, respectively, increasing with the amount of C_{60}-TEGs. The diameter and geometry of the nanofibers were uniform along their length. The fullerene nanoparticles were dispersed reasonably well in the resultant composite nanofibers owing to the homogeneity of the solution.

Figure 4 showed LSCM images of the C_{60}-TEGs encapsulated by the electrospun composite nanofibers. PLLA nanofiber without encapsulating fullerene nanoparticles exhibited no fluorescence properties. The red and bright spots indicated C_{60}-TEGs or their aggregates, distributed uniformly in the composite nanofibers. C_{60}-TEGs was linearly packed and aligned along the axis of the fibers, which could be easily achieved by the application of shear force during the electrospinning process.[28]

The internal structure of the PLLA nanofiber encapsulated with 0 wt.% C_{60}-TEGs and 10 wt.% C_{60}-TEGs were analyzed using TEM, which also confirmed the embedding of the C_{60}-TEGs into the composite nanofiber with core-shell structure. As shown in Figure 5, the dense fullerene nanoparticles C_{60}-TEGs in roughly spherical shape with a diameter of approximately 20 nm were uniformly dispersed in the PLLA nanofiber matrices. Furthermore, C_{60}-TEGs were clearly visible and successfully embedded in the PLLA nanofibers, which consisted of PLLA shell and C_{60}-TEGs as the core. The feasibility of incorporating nanoparticles (both inorganic and organic) into fibers by means of electrospinning for the preparation of nanocomposites had also been confirmed.[22,24,29] When the suspension flowed through a long capillary and
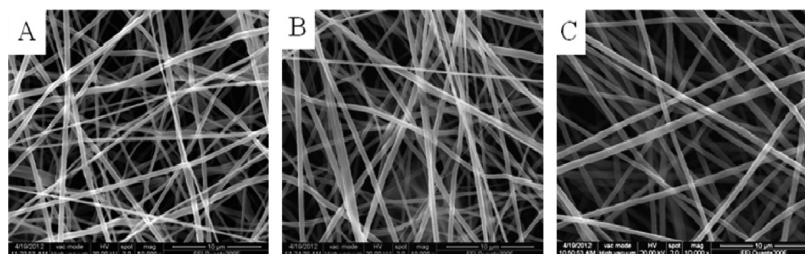

Figure 3. SEM photographs of PLLA nanofibers encapsulated with C_{60}-TEGs: (A) 5 wt.%, (B) 10 wt.%, and (C) 20 wt.%.
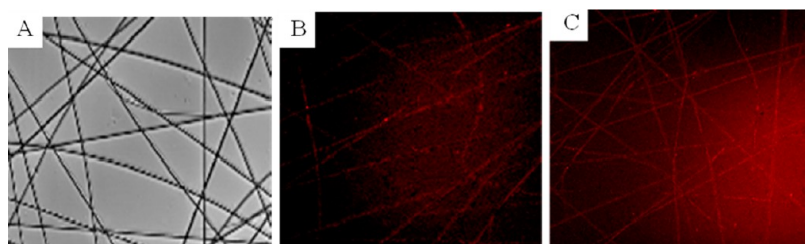
Figure 4. LSCM images PLLA nanofibers encapsulated with C_{60}-TEGs: (A) 0 wt.%, (B) 10 wt.%, and (C) 20 wt.%.
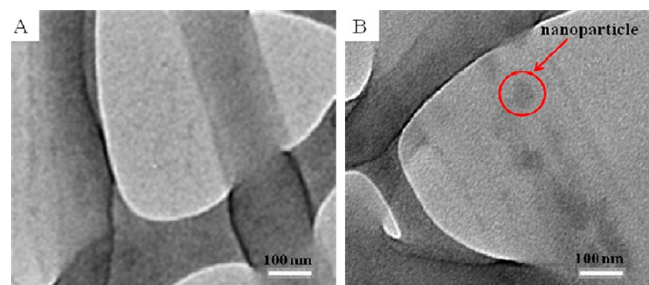

Figure 5. TEM images of PLLA nanofibers encapsulated with (A) 0 wt.% and (B) 10 wt.% C_{60}-TEGs.

formed rapidly expanding and bending fluid jets, the dispersed phase had the tendency to accumulate in the center of the liquid to produce an elongation effect along the direction of the fluid during its flight in the air. This helped nanoparticles settle inside the fibers rather than on their surfaces.[30]

Figure 6 showed the optical observations of the water contact angles on the surface of nanofibrous mats at about 1 s. The
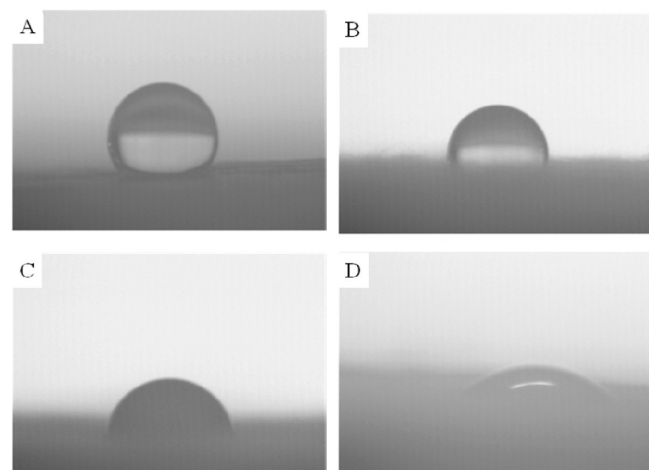

Figure 6. Optical images of water contact angles on the surface of PLLA nanofibers encapsulated with C_{60}-TEGs at 1 s: (A) 0 wt.%, (B) 5 wt.%, (C) 10 wt.%, and (D) 20 wt.%.

water contact angle of the nanofiber contained 20 wt.% C_{60}-TEGs and immediately reached 0° (about 1 s). In the cases of 5 wt.% and 10 wt.% C_{60}-TEGs contained, the water contact angles of the nanofibers were between $68 \pm 0.5°$ and $25 \pm 0.5°$ at 30 s, while the PLLA nanofiber was higher than 120° and almost did not change after 30 s. During the electrospinning process, phase separation between fullerene nanoparticles and PLLA matrix may happen, and some fullerene nanoparticles may transfer to the surface of PLLA matrix due to the volatilization of solvents. In addition, some fullerene nano-

particles were compelled to move onto the nanofibers surface by forces of electric field.[31] The higher the content of nanoparticles loaded in the nanofibers, the more the portion of the nanoparticles came to the nanofiber surfaces. Consequently, it could improve the hydrophilicity properties of the PLLA because fullerene nanoparticles were much more hydrophilic than PLLA.

Mechanical strength was an important factor to be considered as the tissue engineering scaffolds materials. The mean value of mechanical properties of every nanofiber mat was summarized in Table 1. The modulus and the elongation at

Table 1. Mechanical Properties of Nanofibers

PLLA nanofibers	tensile strength/ (MPa) $\pm$ SD	elongation/ (%) $\pm$ SD	modulus/ (MPa) $\pm$ SD
A (blank)	4.1 ± 0.3	112.3 ± 12.4	148.6 ± 7.5
B (contained 5 wt.% C_{60}-TEGs)	3.5 ± 0.4	103.5 ± 13.0	132.8 ± 9.2
C (contained 10 wt.% C_{60}-TEGs)	3.2 ± 0.3	98.9 ± 11.5	126.2 ± 10.1
D (contained 20 wt.% C_{60}-TEGs)	3.0 ± 0.2	94.4 ± 10.8	118.6 ± 8.5
E (contained 10 wt.% C_{70}-TEGs)	3.1 ± 0.3	97.3 ± 12.2	125.0 ± 9.4

break of the nanofibers encapsulated with water-soluble fullerene nanoparticles were 118.6−132.8 MPa and 94.4−103.5%, respectively. The mechanical properties of the nanofibers exhibited a similar tendency, the more the amount of the nanoparticles loaded in nanofibers, the poorer the mechanical properties of the nanofibers. The fullerene nanoparticles were hydrophilic materials, while PLLA was hydrophobic. So the phase compatibility between fullerene nanoparticles and PLLA was poor and might lead to microphase separation, which would result in poorer mechanical properties of PLLA nanofibers encapsulated with fullerene nanoparticles than that of blank PLLA nanofiber (the modulus, 148.6 MPa and the elongation, 112.3%). However, their mechanical properties also reached the requirements of performance for tissue-engineered materials.[32]

***In Vitro* Biological Imaging and Cell Viability Assay.**
Figure 7 showed the fluorescence images of HepG-2 cells which cocultured with PLLA nanofibers encapsulated with water-soluble fullerene nanoparticles at different time. After excitation at 405 nm and collection of 450−650 nm channel, the intense red fluorescence image of HepG-2 cells can be observed in the nucleus, implying a large number of fullerene nanoparticles were endocytosed by HepG-2 cells. Despite the proliferation of HepG-2 cells, the fullerene nanoparticles signal almost displayed in every cell from the fluorescence images, which indicated that there were enough fullerene nanoparticles released from the nanofibers and penetrating into HepG-2
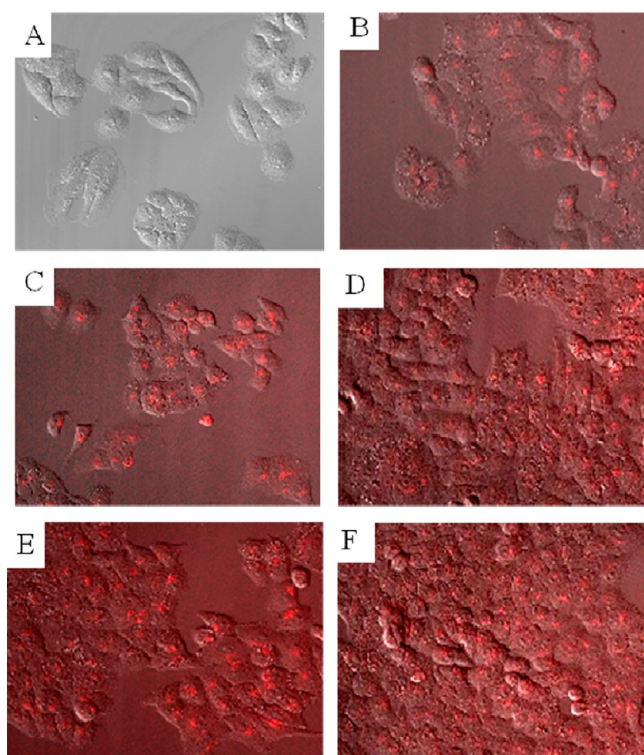
Figure 7. LSCM images of HepG2 cells cocultured with fullerene nanoparticles/PLLA nanofibers: (A) PLLA fiber without fullerene nanoparticles for 24 h, (B) 10 wt.% C_{60}-TEGs for 24 h, (C) 10 wt.% C_{70}-TEGs for 24 h, (D) 10 wt.% C_{60}-TEGs for 48 h, (E) 10 wt.% C_{70}-TEGs for 48 h, and (F) 10 wt.% C_{60}-TEGs for 72 h.

cells for bioimaging. The mechanism of fullerene nanoparticles released from the PLLA matrix was mainly controlled by a diffusion mechanism at the early period, and the fullerene nanoparticles diffused in a way that the fullerene nanoparticle behind always followed the pass-way of the front one. HepG2 cells adhering onto the culture plate, the cell morphology keeping long spindle, nucleus integrity, and cells plumping indicated that the cells grew very well. Furthermore, it was clear in Figure 7 (B-E), the fluorescence intensity and fluorescence imaging effect of C_{70}-TEGs was superior to C_{60}-TEGs, which was consistent with the photoluminescence experimental results.

The cytotoxicities of fullerene nanoparticls and PLLA nanofibers encapsulated with fullerene nanoparticles were determined to be negligible up to a relatively high concentration of 1.0 mg/mL (Figure S2 in the Supporting Information). The cytotoxicities of the nanofibers exhibited a similar tendency, increasing with the amount of fullerene nanoparticles, but the difference between them was very little. The lowest cell viability was 96.9% of the PLLA nanofibers contained 20 wt.% C_{60}-TEGs. These results demonstrated that electrospun nanofibers encapsulated with water-soluble fullerene nanoparticles showed good biocompatibility and low cytotoxicity.

CONCLUSIONS

PLLA nanofibers encapsulated with water-soluble fullerene nanoparticles were successfully prepared by blend electrospinning. The nanofibers were uniform, and their surfaces were reasonably smooth, with the average diameters ranging from 300 to 600 nm. The LSCM and TEM images indicated that fullerene nanoparticles were encapsulated within the composite nanofibers, forming a core−shell structure. The nanofiber scaffolds showed excellent hydrophilic surface due to the addition of the water-soluble fullerene nanoparticles. Their mechanical properties were desirable to tissue-engineered materials. In *in vitro* biological imaging experiments, the intense red fluorescence images of HepG-2 cells could be observed in the nucleus, indicating that fullerene nanoparticles were released from the nanofibers and penetrated into HepG-2 cells. The development of PLLA nanofibers encapsulated with water-soluble fullerene nanoparticles represents a new direction in developing fluorescent biomaterials which could make an impact in bioimaging and drug delivery.

ASSOCIATED CONTENT

$\textcircled{S}$ Supporting Information

The SEM micrographs of blank PLLA nanofiber and PLLA nanofiber encapsulated with 10 wt.% of C_{70}-TEGs), cell viability assay of fullerene nanoparticls, and PLLA nanofibers encapsulated with fullerene nanoparticles. This material is available free of charge via the Internet at http://pubs.acs.org.

AUTHOR INFORMATION

Corresponding Author
*Fax: +86 791 83969561. E-mail: ywchen@ncu.edu.cn.

Author Contributions
§These authors contributed equally.

Notes
The authors declare no competing financial interest.

ACKNOWLEDGMENTS

REFERENCES

(1) Bau, L.; Tecilla, P.; Mancin, F. *Nanoscale* **2011**, *3*, 121−133.
(2) Shen, J.; Sun, L. D.; Zhu, J. D.; Wei, L. H.; Sun, H. F.; Yan, C. H. *Adv. Funct. Mater.* **2010**, *20*, 3708−3714.
(3) Liu, D.; He, X. X.; Wang, K. M.; He, C. M.; Shi, H.; Jian, L. X. *Bioconjugate Chem.* **2010**, *21*, 1673−1684.
(4) Ow, H.; Larson, D. R.; Srivastava, M.; Baird, B. A.; Webb, W. W.; Wiesner, U. *Nano Lett.* **2005**, *5*, 113−117.
(5) Cheng, S. H.; Lee, C. H.; Chen, M. C.; Souris, J. S.; Tseng, F. G.; Yang, C. S.; Mou, C. Y.; Chen, C. T.; Lo, L. W. *J. Mater. Chem.* **2010**, *20*, 6149−6157.
(6) Zrazhevskiy, P.; Sena, M.; Gao, X. H. *Chem. Soc. Rev.* **2010**, *39*, 4326−4354.
(7) Terai, T.; Nagano, T. *Curr. Opin. Chem. Biol.* **2008**, *12*, 515−521.
(8) Wei, G. C.; Yan, M. M.; Ma, L. Y.; Zhang, H. B. *Spectrochim. Acta, Part A* **2012**, *85*, 288−292.
(9) Jeong, J.; Jung, J.; Choi, M.; Kim, J. W.; Chung, S. J.; Lim, S.; Lee, H.; Chung, B. H. *Adv. Mater.* **2012**, *24*, 1999−2003.
(10) Jeong, J.; Cho, M.; Lim, Y. T.; Song, N. W.; Chung, B. H. *Angew. Chem., Int. Ed.* **2009**, *48*, 5296−5299.
(11) Kwag, D. S.; Park, K.; Oh, K. T.; Lee, E. S. *Chem. Commun.* **2013**, *49*, 282−284.
(12) Bhattarai, S. R.; Bhattarai, N.; Yi, H. K.; Hwang, P. H.; Cha, D. I.; Kim, H. Y. *Biomaterials* **2004**, *25*, 2595−2602.
(13) Bhattarai, N.; Li, Z. S.; Edmondson, D.; Zhang, M. Q. *Adv. Mater.* **2006**, *18*, 1463−1467.
(14) Sombatmankhong, K.; Sanchavanakit, N.; Pavasant, P.; Supaphol, P. *Polymer* **2007**, *48*, 1419−1427.
(15) Wei, M.; Kang, B.; Sung, C.; Mead, J. *Macromol. Mater. Eng.* **2006**, *291*, 1307−1314.

(16) Armentano, I.; Dottori, M.; Fortunati, E.; Mattioli, S.; Kenny, J. M. *Polym. Degrad. Stab.* **2010**, *95*, 2126−2146.

(17) Noh, H. K.; Lee, S. W.; Kim, J. M.; Oh, J. E.; Kim, K. H.; Chung, C. P.; Choi, S. C.; Park, W. H.; Min, B. M. *Biomaterials* **2006**, *27*, 3934−3944.

(18) Meng, C.; Xiao, Y.; Wang, P.; Zhang, L.; Liu, Y.; Tong, L. *Adv. Mater.* **2011**, *23*, 3770−3774.

(19) Kim, K.; Luu, Y. K.; Chang, C.; Fang, D.; Hsiao, B. S.; Chu, B.; Hadjiargyrou, M. *J. Controlled Release* **2004**, *98*, 47−56.

(20) Sun, X. B.; Zhang, L. F.; Cao, Z. B.; Deng, Y.; Liu, L.; Fong, H.; Sun, Y. Y. *ACS Appl. Mater. Interfaces* **2010**, *2*, 952−956.

(21) Li, C.; Vepari, C.; Jin, H. J.; Kim, H. J.; Kaplan, D. L. *Biomaterials* **2006**, *27*, 3115−3124.

(22) Lu, X. F.; Wang, C.; Wei, Y. *Small* **2009**, *5*, 2349−2370.

(23) Yoo, H. S.; Kim, T. G.; Park, T. G. *Adv. Drug Delivery Rev.* **2009**, *61*, 1033−1042.

(24) Dhandayuthapani, B.; Poulose, A. C.; Nagaoka, Y.; Hasumura, T.; Yoshida, Y.; Maekawa, T.; Kumar, D. S. *Biofabrication* **2012**, *4*, 025008.

(25) Ma, Z.; Chen, F.; Zhu, Y. J.; Cui, T.; Liu, X. Y. *J. Colloid Interface Sci.* **2011**, *359*, 371−379.

(26) Liu, X. H.; Ma, P. X. *Biomaterials* **2010**, *31*, 259−269.

(27) Kakinoki, S.; Uchida, S.; Ehashi, T.; Murakami, A.; Yamaoka, T. *Polymers* **2011**, *3*, 820−832.

(28) Lim, J. M.; Moon, J. H.; Yi, G. R.; Heo, C. J.; Yang, S. M. *Langmuir* **2006**, *22*, 3345−3349.

(29) Teo, W. E.; Ramakrishna, S. *Compos. Sci. Technol.* **2009**, *69*, 1804−1817.

(30) Qi, H. X.; Hu, P.; Xu, J.; Wang, A. J. *Biomacromolecules* **2006**, *7*, 2327−2330.

(31) Li, X. Q.; Su, Y.; Liu, S. P.; Tan, L. J.; Mo, X. M.; Ramakrishna, S. *Colloids Surf., B* **2010**, *75*, 418−424.

(32) Li, W. J.; Laurencin, C. T.; Caterson, E. J.; Tuan, R. S.; Ko, F. K. *J. Biomed. Mater. Res.* **2002**, *60*, 613−621.